

Published in final edited form as:

Gastroenterology. 2012 October ; 143(4): . doi:10.1053/j.gastro.2012.06.036.

Deactivation of Hepatic Stellate Cells during Liver Fibrosis Resolution in Mice

Juliane S. Troeger^{#1}, Ingmar Mederacke^{#1}, Geum-Youn Gwak¹, Dianne H. Dapito^{1,2}, Xueru Mu¹, Christine C. Hsu¹, Jean-Philippe Pradere¹, Richard A. Friedman^{3,4}, and Robert F. Schwabe^{1,2}

¹Department of Medicine, Columbia University, College of Physicians and Surgeons, New York, NY

²Institute of Human Nutrition, Columbia University, New York, NY

³Herbert Irving Comprehensive Cancer Center, Columbia University, New York, NY 10032, USA

⁴Center for Computational Biology and Bioinformatics, Columbia University, New York, NY 10032, USA

These authors contributed equally to this work.

Abstract

Background & Aims—Activated hepatic stellate cells (HSCs), the main fibrogenic cell type of the liver, undergo apoptosis after cessation of liver injury, thereby contributing to the resolution of liver fibrosis. In this study, we investigated whether HSC deactivation constitutes an additional mechanism of liver fibrosis resolution.

Methods—HSC activation and deactivation were investigated by single cell PCR and genetic tracking in transgenic mice expressing tamoxifen-inducible CreER under control of the endogenous vimentin promoter (VimCreER).

Results—Single cell quantitative PCR demonstrated activation of virtually the entire HSC population in fibrotic livers, and a gradual decrease of HSC activation during fibrosis resolution, indicating deactivation of HSCs. VimCreER marked activated HSCs, demonstrated by a 6- to 16-fold induction of a membrane-bound green fluorescent protein (mGFP) Cre-reporter following injection of carbontetrachloride (CCl₄) in both liver and isolated HSCs, and a shift in localization of mGFP-marked HSCs from perisinusoidal to fibrotic septa. Tracking of mGFP-positive HSCs revealed the persistence of 40–45% of mGFP expression in livers and isolated HSCs 30–45 days after cessation of CCl₄, despite normalization of fibrogenesis parameters, thereby confirming reversal of HSC activation. After fibrosis resolution, mGFP expression was observed again in desmin-positive perisinusoidal HSCs; no mGFP expression was detected in hepatocytes or

Correspondence: Robert F. Schwabe; Department of Medicine, Columbia University, College of Physicians & Surgeons, Russ Berrie Pavilion, Room 415, 1150 St. Nicholas Ave, New York, NY 10032; rfs2102@columbia.edu; Tel: (212) 851-5462, Fax: (212) 851-5461.

Author contributions: Juliane S. Troeger generated transgenic mice and was involved in data acquisition (4×CCl₄ model), analysis and interpretation of data, statistical analysis and experimental design and drafting of the manuscript. Ingmar Mederacke was involved in acquisition (4×CCl₄ model, 8×CCl₄ model, TAA model and characterization of reverted HSCs), analysis and interpretation of data, statistical analysis, experimental design and drafting of the manuscript. Geum-Youn Gwak, Dianne H. Dapito, Jean-Philippe Pradere, Xueru Mu and Christine C. Hsu were involved in data acquisition and analysis. Richard Friedman performed microarray data analysis. Robert F. Schwabe was responsible for overall study concept and design, drafting of the manuscript, supervised the study and performed data analysis.

Disclosures: No conflicting interests exist.

cholangiocytes, thereby excluding mesenchymal-epithelial transition. Notably, reverted HSCs remained in a primed state, with higher responsiveness to profibrogenic stimuli.

Conclusion—In mice, reversal of HSC activation contributes to the termination of fibrogenesis during fibrosis resolution but results in higher responsiveness of reverted HSCs to recurring fibrogenic stimulation.

Introduction

Hepatic stellate cells (HSCs) are considered the main fibrogenic cell type of the liver. In response to injury, HSCs undergo a well-characterized activation process during which they lose their characteristic vitamin A and lipid stores, and obtain a myofibroblastic phenotype^{1,2}. This activation process is driven by two cytokines, transforming growth factor β , and platelet-derived growth factor, leading to increased expression of contractile filaments such as α -smooth muscle actin (α SMA) and extracellular matrix (ECM) proteins such as collagen I.^{1,2} While the loss of vitamin A storage is a characteristic feature of HSC activation, it does not affect HSC activation as apparent by the normal activation of HSCs lacking the characteristic retinoid and lipid droplets.³

The principal ability of the fibrotic liver to revert to a less fibrotic or even normal architecture has been convincingly demonstrated over the last two decades in both rodents^{4–6} and in patients following successful treatment of various underlying diseases.^{7–12} Previous studies have elegantly demonstrated that the reversal of liver fibrosis leads to a reduction of myofibroblasts, and that this reduction of myofibroblasts is accompanied by increased myofibroblast apoptosis.⁶ Moreover, increasing myofibroblast apoptosis by pharmacological approaches accelerates fibrosis resolution suggesting a causative contribution of apoptosis to this process.¹³ While apoptosis is one key mechanism through which activated myofibroblasts are removed from fibrotic and cirrhotic livers, it is also conceivable that activated myofibroblasts may re-differentiate and return to a quiescent phenotype. Here we employ both single cell PCR and genetic tracking to test the hypothesis that activated HSCs are capable of deactivating.

Methods

Generation of Vim-CreER mice

A CreER^{Frt}Neo^{Frt} cassette was PCR-amplified from a p451 plasmid¹⁴ with 60 bp overhangs homologous to the upstream and downstream sequence surrounding ATG site of the mouse vimentin gene. The PCR product was inserted into a BAC containing the mouse vimentin gene by recombineering. Following removal of the Neo cassette by arabinose-induced flippase, BAC DNA was microinjected in the pronucleus of fertilized CBA \times C57BL/6J oocytes. One out of three founders showed strong Vim-CreER activity after tamoxifen injection. For experiments, mice were bred once with Balb/c mice to generate male Vim-CreER⁺ mTom/mGFP⁺ mice used for experiments. Genotyping for Vimentin-Cre was done using forward primer 5'-CCCCTTCCTCACTTCTTTCC and reverse primer 5'-ATGTTTAGCTGGCCCAAATG. All animal procedures were in accordance to guidelines by the National Institutes of Health, and approved by the Institutional Animal Care and Use Committee at Columbia University.

Fibrosis induction, tamoxifen injection and fibrosis reversal

Hepatic fibrosis was induced by four to eight intraperitoneal injections of carbontetrachloride (CCl₄, 0.5 μ l/g, dissolved in corn oil at a ratio of 1:3). For some experiments, mice were treated with 12–18 intraperitoneal injections of thioacetamide (TAA) over 4–6 weeks at increasing TAA concentrations (1st dose: 50 mg/kg, 2nd dose: 100

mg/kg, 3rd to 6th dose: 200 mg/kg, all following doses: 300 mg/kg). For some experiments, mice underwent ligation of the common bile duct as previously described.^{15,16} Vim-CreER activity was induced by 6 intraperitoneal injections of tamoxifen (2 mg/mouse dissolved in corn oil) starting 3 days after the first CCl₄ injection and ending one day before the last CCl₄ injection.

HSC isolation

HSCs were isolated as previously described using pronase-collagenase perfusion followed by Nycodenz gradient centrifugation^{17,18}, and in some cases additionally purified by Vitamin A-autofluorescence-based FACS sorting.

HSC activation in cell culture

To compare the activation of normal and reverted HSCs in response to fibrogenic stimuli, HSCs were either isolated from untreated Balb/c mice or age-matched Balb/c mice that received 4 injections of CCl₄ (0.5 μ l/g i.p.) with the last injection occurring 45 days before isolation. A portion of the cells were lysed directly without any plating or culture (quiescent HSCs) whereas all other cells were plated in 10% FBS containing media for 4 hours followed by additional culture in media containing 0.1% FBS for 48h in the presence or absence of recombinant human TGF β (2.5 ng/ml) or recombinant human PDGF (20 ng/ml), or in media containing 10% FBS.

Additional experimental procedures are described in the Supplemental Materials.

Results

Activation of HSCs in the injured liver at a single cell level

To determine whether activated HSCs may deactivate, we first compared fibrogenic gene expression in CCl₄-injured livers and HSCs at different time points after cessation of injury to pre- and peak-injury levels. Following four injections of CCl₄, fibrogenic gene expression in whole liver was elevated two days after the last injection, and gradually returned to normal levels with almost normalized levels of fibrogenic gene expression 30 days after the last CCl₄ injection (Fig. 1A). This regimen also induced significant histological fibrosis that almost completely resolved 30 days after the last CCl₄ injection (Fig. 1B). Similar to whole liver, we also found peak fibrogenic gene expression 1 and 2 days after the last CCl₄ injection in isolated HSCs, strongly decreased levels already 3 and 5 days after the last CCl₄ injection and virtually normal levels at days 15 and 30 post-CCl₄ (Fig. 1C and Suppl. Fig. 1). To investigate the hypothesis that activated HSCs may “de-activate” and return to a quiescent state following cessation of liver injury, it is helpful to know the proportion of HSCs that undergo activation in the fibrotic liver. Current mRNA and protein-based approaches only measure HSC activation in the entire cell population and may suggest activation of an entire population even when only a small subpopulation activates and the remainder stays in a quiescent state. To address this question, we employed FACS sorting and single cell PCR for quantification of fibrogenic gene expression in HSCs. Single cell PCR revealed more than 90% of HSCs ($p < 0.01$) were in an activated state 2 days after the last CCl₄ injection as demonstrated by at least 10-fold expression of Col1a1 and higher Col1a1 expression than each single quiescent HSC investigated (Fig. 1D).

Hepatic stellate cells gradually de-activate

After having determined that virtually all HSCs are in an activated state in the fibrotic liver, we next investigated HSC deactivation by single cell qPCR. If HSC inactivation occurred only by apoptosis, the fraction of activated HSCs should consistently decrease and the fraction of quiescent HSCs replacing activated HSCs should increase during the recovery

period - but the degree of activation should not decrease in activated HSCs that persist. In contrast, HSCs should gradually reduce profibrogenic gene expression during the recovery period and none or few cells should remain in a highly activated state if they were able to deactivate. In both settings, gene expression in the entire population would decrease but the gene expression pattern in single HSCs would look drastically different. By single cell qPCR analysis, we found that expression of the well-established HSC activation markers *Col1a1* and *TIMP1* gradually and constantly decreased in virtually all HSCs over the entire recovery period between day 2 and day 15 post-CCl₄ (Fig.1D). These data strongly suggest that virtually all HSCs in the recovering liver that are not removed by apoptosis are HSCs undergoing deactivation. To validate these findings, we subjected mice to TAA-induced liver injury as a second model of liver fibrosis. Although the extent of *Col1a1* upregulation was lower than in the CCl₄ model, we observed a similar gradual deactivation of HSCs after cessation of TAA again suggesting reversal of HSC activation (Suppl. Fig. 2A).

Vim-CreER marks myofibroblasts

To determine HSC deactivation by a second method and provide quantification of the percentage of HSCs undergoing deactivation during fibrosis regression, we generated a novel BAC-transgenic mouse to mark and track myofibroblasts during the injury and resolution phase. We chose CreER expression to be driven by vimentin, an intermediate filament that is expressed in mesenchymal cell populations with very high expression in myofibroblasts.¹⁹ In the liver, vimentin is predominantly expressed in HSCs but may also be found in vascular smooth muscle cells and portal fibroblasts^{20,21} To generate a BAC transgenic mouse driven by the vimentin promoter, we inserted a CreER cassette in a BAC containing the mouse vimentin locus (Vim-CreER, Suppl.Fig.3). Using the mTommGFP Cre reporter mouse²² in which mTom is expressed in the absence of Cre activity and mGFP in cells with Cre activity (Fig.2A), we analyzed VimCreER-marked cell populations in the liver and various other organs. Whereas there was only minimal expression of mGFP in the liver after 6 injections of tamoxifen, stomach, small intestine, colon and kidney showed abundant expression of mGFP (Fig.2B). We also determined whether Vim-CreER-driven expression was detectable in other hepatic cell populations, in particular in endothelial cells, which are known to express vimentin, albeit at lower levels. In the liver, we found no Vim-CreER-driven mGFP expression in CD31-expressing endothelial cells (Suppl.Fig.4) consistent with a previous study.²¹ Similarly, there was proximity but no overlap between mGFP and CD31 in other organs including stomach, small intestine and colon (Suppl.Fig.4). Also, macrophages expressing F4/80 were not marked by Vim-CreER-induced mGFP (Suppl.Fig.5). These findings demonstrate that VimCreER is a useful tool to broadly and specifically label myofibroblast and are consistent with the notion that the normal liver contains only few myofibroblasts whereas myofibroblasts are an integral part of many other organs. Next, we induced liver fibrosis in Vim-CreER mice by two different methods, CCl₄ injection and bile duct ligation. Vim-CreER strongly induced mGFP expression in patterns typical for myofibroblast localization after CCl₄-induced liver injury (Fig.2C). In the bile duct ligation model, mGFP expression was also significantly induced but to a lesser extent than in the CCl₄ model (Suppl.Fig.6). Due to the stronger labeling in the CCl₄ model, we focused on this model for the remainder of our study on fibrosis regression. Next, we confirmed that Vim-CreER-mediated mGFP expression matched endogenous vimentin expression by confocal microscopy, which demonstrated co-localization of Vim-CreER-induced mGFP expression and endogenous vimentin in both fibrotic liver and the intestinal tract (Fig.2D).

Reversal of activated HSCs during fibrosis regression

To determine whether activated myofibroblasts may return to a quiescent phenotype, we subjected Vim-CreER mice to CCl₄-induced liver fibrosis while inducing CreER with

tamoxifen and analyzed mGFP expression pre-injury, at peak injury as well as 15 and 30 days after cessation of CCl₄ treatment (Fig.3A). mGFP expression increased from 0.2% of the liver area in untreated livers to 3.2% in CCl₄-treated livers at day 2 (Fig.3B–C). Despite normalization of fibrosis parameters (Fig.3D), mGFP expression did not return to pre-treatment levels but persisted at 1.5% and 1.4% at day 15 and day 30 post-CCl₄ (Fig.3B–C), respectively, suggesting that 40% of hepatic myofibroblasts reverted to a quiescent state. Moreover, the localization of mGFP-positive cells changed from being largely in prototypical CCl₄-induced fibrotic septa to being in the typical perisinusoidal localization of quiescent HSCs as indicated by arrows (Fig.3B). To confirm that the observed labeling of cells in the fibrotic liver occurred indeed in HSCs, we isolated HSCs from CCl₄-treated fibrotic livers at various time points and analyzed mGFP expression by FACS analysis of Vitamin A-positive HSCs. While only 4.6% of quiescent HSCs expressed mGFP, the expression of mGFP increased strongly to 27.5% of HSCs 2 days after CCl₄ treatment (Fig. 4A–B). Similar to our analysis in whole liver, HSCs maintained mGFP expression after cessation of injury with 13.8% of HSCs still expressing mGFP 30 days after injury (Fig.4B). Quantitative real-time PCR of mGFP-negative and mGFP-positive HSCs demonstrated both populations had de-activated (Fig.4C–D) thus proving that these cells were not cells that remained in activated state in late stages of resolution but that they reverted from an

activated to a quiescent state. The reversal rate, calculated as $\text{Reversal} = \frac{d30 - \text{untreated}}{d2 - \text{untreated}}$, was 40% and thus identical to the rate of reverted myofibroblasts observed by confocal microscopy of liver sections (Fig.3C). To further confirm these findings, we additionally plated isolated HSCs and quantified cells that were both Vitamin A autofluorescent and expressed mGFP as visualized by fluorescent microscopy (Fig.4E). Again, mGFP expression was retained in HSCs isolated 30 days after cessation of CCl₄ treatment with 3.6% of HSCs from untreated livers being positive, 23% from day 2 CCl₄-treated livers positive and 12.5% from day 30 CCl₄-treated liver positive translating to a reversal rate of 45% (Fig.4F). As we analyzed mGFP expression in mice receiving no CCl₄ at a time point corresponding to day 2 post-CCl₄, we wanted exclude that we underestimated the mGFP signal due to a potential expansion of the mGFP-marked HSC population between day 2 and day 30. For this purpose, we additionally compared liver sections and HSCs from untreated and CCl₄-treated mice that both were sacrificed 30 days after the last CCl₄ injection (Suppl.Fig.7). In this experimental setting, we again found a significant increase in mGFP-positive liver area and mGFP-positive HSCs and a highly similar induction of mGFP expression in CCl₄-treated mice (Suppl. Fig.7). To determine whether activated HSCs also revert to a quiescent phenotype in more established fibrosis, mice were treated with CCl₄ for one month followed by recovery for 45 days. Similar to our data in the shorter term fibrosis model, we also saw reversal of activated HSCs with a reversal rate of about 29% and 37–43% as determined in whole liver sections and isolated HSCs, respectively (Suppl. Fig.8). We additionally employed liver fibrosis induced by 18 injections of thioacetamide (TAA) as a second long-term model to confirm reversal of HSC activation. In this model, we also observed a significant increase of mGFP labeling at peak fibrosis and a statistically significant retention of the mGFP label in HSCs 45 days after the last TAA injection, thus confirming our findings in the CCl₄ model (Suppl. Fig.2B). To exclude that Vim-CreER expressing cells might have been recruited from the bone marrow during recovery and that the observed mGFP signal represents recruitment from bone marrow rather than HSC reversal, we performed bone marrow transplantation of Vim-CreER positive bone marrow in Vim-CreER negative recipients and treated mice with CCl₄. We saw only few scattered GFP positive cells in the liver representing less than 0.5% of all cells both 2 days and 30 days after CCl₄ treatment and no mGFP positive HSCs (Suppl. Fig. 9A) thus excluding a contribution of the bone marrow to mGFP-positive cell populations at peak fibrosis or during fibrosis resolution (Suppl. Fig. 9B–C). In summary, we observe retention of mGFP

expression and reversal of activation in 40–45% of myofibroblasts/HSCs by three different approaches including confocal microscopy, FACS analysis and manual counting.

Vim-CreER marked myofibroblasts do not undergo mesenchymal-epithelial transition

To further confirm that activated myofibroblasts revert to becoming HSCs, we performed confocal microscopy of liver sections stained with desmin, a well-known marker of HSCs in the normal liver. While there was little mGFP staining in the normal liver, the few areas of mGFP positive cells showed clear overlap with desmin staining (Fig.5A). Expectedly, mGFP expression was increased at day 30 post injury, and all mGFP-positive cells were also desmin-positive (Fig.5A) suggesting that activated mGFP-labeled myofibroblasts indeed re-differentiated into HSCs. Previous studies have suggested that HSCs may also be capable to differentiate into epithelial cells²³. To determine whether activated mGFP-labeled myofibroblasts may also differentiate into hepatocytes or cholangiocytes, we performed confocal microscopy for HNF4 α and pankheratin. Careful analysis in multiple animals and sections demonstrated no mGFP-positive cells with typical hepatocyte nuclear shape or positive HNF4 α staining (Fig.5B). Similarly, there was no overlap between mGFP expression and keratin-positive bile ducts (Fig.5C) demonstrating that Vim-CreER labeled myofibroblasts do not differentiate into hepatocytes or cholangiocytes in CCl₄-induced liver fibrosis.

Reverted HSCs are more susceptible to subsequent activation

To determine whether previous activation and subsequent deactivation might affect HSC biology, we compared fibrogenic responses between treatment-naïve quiescent HSCs and HSCs that had been isolated 45 days after the last CCl₄ treatment and thus undergone reversion to a quiescent phenotype. To exclude adaptations of other hepatic cell types to injury or metabolism of CCl₄ in response to repeated injury, we isolated HSCs and activated them in cell culture dishes by exposing them to well-established fibrogenic stimuli including TGF β , PDGF and 10% fetal bovine serum (FBS). Expression of the activation marker α SMA was similar in freshly unplate quiescent HSCs and HSCs kept in 0.1% FBS under baseline conditions. However, when HSCs were stimulated with TGF β , PDGF or 10% FBS for 48h, reverted HSCs showed a higher level of activation than treatment-naïve quiescent HSCs as demonstrated by increased α SMA protein expression (Fig. 6A–B) as well as by increased Col1a1 and Acta2 mRNA expression (Fig. 6C–D). Microarray analysis demonstrated 37 significantly changed genes but did not reveal profound changes in gene expression or activation of pathways that might explain a higher responsiveness to specific fibrogenic stimuli in reverted HSCs (Fig.6E, Suppl. Tables 1–2, Suppl. Fig.10). Instead, microarray and qPCR analysis indicated that reverted HSCs did not completely reach the quiescent status of qHSCs: Genes that were elevated in reverted HSCs in comparison to qHSCs were also upregulated in HSCs at peak fibrosis, and genes that had lower expression in reverted HSCs were downregulated in HSCs at peak fibrosis (Fig. 6F), consistent with an incomplete return of reverted HSCs to quiescence. Thus, it is most likely that reverted HSCs, despite not having significantly elevated levels of markers such as α SMA or Col1a1, retain a pre-activated state and therefore readily activate in response to recurring fibrogenic stimuli.

Discussion

Removal of hepatic myofibroblasts by apoptosis is considered the key mechanism that reduces the number of activated myofibroblasts and allows the liver to return to normal architecture.⁶ Here we provide evidence that reversal of hepatic myofibroblasts to a quiescent state represents a second mechanism that contributes to the regression of liver fibrosis. Our study used two complementary approaches, single cell qPCR and genetic cell

fate tracking, to determine reversal of activated HSCs to a quiescent phenotype. Single cell qPCR clearly demonstrated a gradual and constant decline of HSC activation parameters after cessation of CCl₄-induced liver injury consistent with deactivation of HSCs. The single cell PCR approach does not exclude HSC apoptosis, and does not allow to determine the percentage of reverting HSCs as apoptotic HSCs cannot be isolated and quantified in the HSC isolate. As a second line of evidence for HSC reversal, we used genetic cell fate tracking in BAC-transgenic Vimentin-CreER mice. Our results show faithful tracking of myofibroblasts in various organs including the digestive tract and the fibrotic liver, and mGFP expression increased when myofibroblasts accumulated during liver fibrosis. Interestingly, despite normalization of fibrosis parameters, CCl₄-induced mGFP persisted to a similar degree in liver sections and isolated HSCs demonstrating a reversal rate of about 40–45%. These results suggest that HSC apoptosis and deactivation are both major contributors to the reversal of murine liver fibrosis. Further studies are required to define the pathways that determine whether HSCs deactivate or undergo apoptosis. It is well known that HSC numbers increase in the fibrotic livers. One could speculate that the removal of HSCs by apoptosis not only serves to reduce fibrogenesis but also to restore the number of HSCs to the pre-injury state. As we used a tamoxifen-inducible Cre mouse and did not continue to give tamoxifen during the resolution phase, we can exclude that another cell population such as newly generated HSCs might represent this mGFP-positive cell population. We also did not see a hepatic accumulation of mGFP-positive bone-marrow derived cells at peak fibrosis or after fibrosis resolution further excluding the possibility that mGFP-positive cells in the reverted liver might represent cell populations recruited from a mGFP-positive source in the bone marrow rather than reverted HSCs. We can also exclude that mGFP labeled HSCs remaining in the liver at day 30 constitute a cell population that remains highly activated as fibrogenesis markers in the whole liver as well as in sorted mGFP-positive HSC were $\approx 95\%$ lower than a peak activation, almost reaching baseline levels. Moreover, we found that “de-activated” HSCs returned from being localized next to fibrotic septa to their characteristic perisinusoidal location within the entire lobule. It is well known that chemokines play an important role in controlling and directing the migration of HSCs to the site of injury.^{24,25} Further studies are required to determine the nature of the homing signal that keeps or returns HSCs in their perisinusoidal localization. It is likely that this signal constitutes factors present in the space of Disse that are either lost in the injured liver or overridden by chemoattractant signals from the site of injury. A similar migration of pericytes from capillaries towards the interstitium with subsequent differentiation into myofibroblasts has also been shown in the kidney²⁶. While we have proven the principal ability of HSCs to return to deactivate after cessation of injury, it is not clear whether this is true for all settings and how relevant this mechanism may be for patients with liver fibrosis or cirrhosis. Although we also saw persistence of mGFP in more prolonged fibrosis models, i.e. after eight CCl₄ or eighteen TAA injections, human fibrogenesis is a process that develops over years and thus differs from rodent fibrosis models. We also cannot exclude that activated HSCs may eventually lose the ability to revert to a quiescent phenotype once they have crossed a certain threshold of activation and reached a “point of no return”, and then either apoptose or persist in the liver. Also, it is possible that undegradable ECM persists in the liver after cessation of injury,^{27,28} and that this persisting ECM may keep some myofibroblasts in an activated state and unable to deactivate. Accordingly, lysyl oxidase-mediated and tissue transglutaminase-independent ECM crosslinking not only affects liver stiffness but also myofibroblast activation.^{28–30} Since lipid droplet-containing activated HSCs can be isolated in high numbers from human livers with advanced fibrosis or even cirrhosis,³¹ it can be speculated that a population of activated lipid droplet-containing HSCs similar to that investigated in our study exists in most human patients, and that a reversal of activation in these cells may also occur in patients after cessation of injury. The number of reverting HSCs was 35–45% in our murine study, but may be lower in humans and will be difficult to quantify. A recently published study also provides strong evidence

for the occurrence of HSC reversal and a similar percentage of HSC reversal³² further emphasizing the relevance of this phenomenon.

It is conceivable that HSC deactivation is actively regulated, or a consequence of decreased exposure to fibrogenic mediators after cessation of injury. Although we have performed extensive microarray analysis of HSCs isolated at various time points after cessation of injury (data not shown), we have been unable to identify a mediator or pathway that actively returns activated HSCs to a quiescent phenotype. We observed that all genes that were up- or downregulated at day 2 post-CCl₄ approached pre-injury levels at d5 and d12 but did not find potential “resolution genes” whose up- or downregulation started only after peak fibrosis and was maximally changed during the resolution phase (data not shown). Therefore, we consider it most likely that the decreased availability of fibrogenic mediators after cessation of injury is the principal driver of HSC deactivation. This implies that anti-fibrogenic therapies should in principle not only prevent new activation of HSCs but also induce deactivation of already activated HSCs. This finding has potential clinical relevance as it predicts that HSC-targeting anti-fibrotic therapies may not only be used as preventative strategies but should, in principle, be even effective in settings in which significant fibrosis has already developed. This knowledge may be important for the future development of drugs that target the HSC activation process rather than the underlying disease.

Reverted HSCs display considerable biological differences to quiescent HSCs despite their almost complete deactivation with only marginal but non-significant elevation of activation parameters 45 days after the last CCl₄ injection. Notably, reverted HSCs were much more responsive to fibrogenic stimuli including TGFβ and PDGF than quiescent HSCs that had not been previously activated. These results are similar to a study published during the preparation of this manuscript³². Microarray analysis and qPCR did not reveal candidates that render reverted HSCs more responsive to fibrogenic stimuli but suggests that gene expression of reverted HSCs does not fully return to the status of qHSCs thus allowing them to reactivate more rapidly. Although we observed a profound downregulation of Hspa1a and Hspa1b mRNA at peak fibrosis (data not shown) as reported in a previous study³², we did not observe the reported increase of Hspa1a and Hspa1a during the early resolution stage (data not shown) nor did our microarray analysis reveal a difference in Hspa1a and Hspa1b levels between quiescent and reverted HSCs. It is likely that hepatic responses to recurring fibrogenic stimulation also depend on other hepatic cell populations and are modulated by the susceptibility of hepatocytes and the response of inflammatory cells to recurrent injury.

We also did not observe any evidence of mesenchymal-epithelial transition (MET) after cessation of liver injury. These results are different from a previous study in which HSCs were tracked by GFAP-Cre and fibrosis was induced by a choline-deficient, ethionine-supplemented diet,²³ but similar to a recent study which employed CCl₄ for fibrosis induction in GFAP-Cre mice and observed no MET.³³

In summary, our study shows deactivation of roughly half the HSC population during liver fibrosis regression and higher responsiveness of reverted HSCs to recurrent profibrogenic stimulation.

Supplementary Material

Refer to Web version on PubMed Central for supplementary material.

Acknowledgments

Grant support: This study was supported by grants U54CA126513 (PI of Project 2: RFS) and U54CA163111. Ingmar Mederacke was supported by the German Research Foundation (ME 3723/1-1). Dianne Dapito was

supported by 1F31DK091980. Jean-Philippe Pradere was supported by a postdoctoral fellowship from the American Liver Foundation.

Abbreviations

α-SMA	α smooth muscle actin
CCl₄	carbon tetrachloride
ECM	extracellular matrix
mGFP	membrane-bound green fluorescent protein
HSC	hepatic stellate cell
qPCR	quantitative real-time PCR
TAA	thioacetamide
VimCreER	Vimentin-CreER

References

1. Bataller R, Brenner DA. Liver fibrosis. *J Clin Invest*. 2005; 115:209–18. [PubMed: 15690074]
2. Friedman SL. Hepatic stellate cells: protean, multifunctional, and enigmatic cells of the liver. *Physiol Rev*. 2008; 88:125–72. [PubMed: 18195085]
3. Kluwe J, Wongsiriroj N, Troeger JS, et al. Absence of hepatic stellate cell retinoid lipid droplets does not enhance hepatic fibrosis but decreases hepatic carcinogenesis. *Gut*. 2011; 60:1260–8. [PubMed: 21278145]
4. Morcos SH, Khayyal MT, Mansour MM, et al. Reversal of hepatic fibrosis after praziquantel therapy of murine schistosomiasis. *Am J Trop Med Hyg*. 1985; 34:314–21. [PubMed: 3985273]
5. Abdel-Aziz G, Lebeau G, Rescan PY, et al. Reversibility of hepatic fibrosis in experimentally induced cholestasis in rat. *Am J Pathol*. 1990; 137:1333–42. [PubMed: 2260623]
6. Iredale JP, Benyon RC, Pickering J, et al. Mechanisms of spontaneous resolution of rat liver fibrosis. Hepatic stellate cell apoptosis and reduced hepatic expression of metalloproteinase inhibitors. *J Clin Invest*. 1998; 102:538–49. [PubMed: 9691091]
7. Hammel P, Couvelard A, O'Toole D, et al. Regression of liver fibrosis after biliary drainage in patients with chronic pancreatitis and stenosis of the common bile duct. *N Engl J Med*. 2001; 344:418–23. [PubMed: 11172178]
8. Kweon YO, Goodman ZD, Dienstag JL, et al. Decreasing fibrogenesis: an immunohistochemical study of paired liver biopsies following lamivudine therapy for chronic hepatitis B. *J Hepatol*. 2001; 35:749–55. [PubMed: 11738102]
9. Poynard T, McHutchison J, Manns M, et al. Impact of pegylated interferon alfa-2b and ribavirin on liver fibrosis in patients with chronic hepatitis C. *Gastroenterology*. 2002; 122:1303–13. [PubMed: 11984517]
10. Muretto P, Angelucci E, Lucarelli G. Reversibility of cirrhosis in patients cured of thalassemia by bone marrow transplantation. *Ann Intern Med*. 2002; 136:667–72. [PubMed: 11992302]
11. Farci P, Roskams T, Chessa L, et al. Long-term benefit of interferon alpha therapy of chronic hepatitis D: regression of advanced hepatic fibrosis. *Gastroenterology*. 2004; 126:1740–9. [PubMed: 15188169]
12. Dixon JB, Bhathal PS, Hughes NR, et al. Nonalcoholic fatty liver disease: Improvement in liver histological analysis with weight loss. *Hepatology*. 2004; 39:1647–54. [PubMed: 15185306]
13. Wright MC, Issa R, Smart DE, et al. Gliotoxin stimulates the apoptosis of human and rat hepatic stellate cells and enhances the resolution of liver fibrosis in rats. *Gastroenterology*. 2001; 121:685–98. [PubMed: 11522753]
14. Quante M, Marrache F, Goldenring JR, et al. TFF2 mRNA transcript expression marks a gland progenitor cell of the gastric oxyntic mucosa. *Gastroenterology*. 2010; 139:2018–2027. e2. [PubMed: 20708616]

15. Kluwe J, Pradere JP, Gwak GY, et al. Modulation of hepatic fibrosis by c-Jun-N-terminal kinase inhibition. *Gastroenterology*. 2010; 138:347–59. [PubMed: 19782079]
16. Seki E, De Minicis S, Gwak GY, et al. CCR1 and CCR5 promote hepatic fibrosis in mice. *J Clin Invest*. 2009; 119:1858–70. [PubMed: 19603542]
17. Dapito DH, Mencin A, Gwak GY, et al. Promotion of Hepatocellular Carcinoma by the Intestinal Microbiota and TLR4. *Cancer Cell*. 2012; 21:504–16. [PubMed: 22516259]
18. Seki E, De Minicis S, Osterreicher CH, et al. TLR4 enhances TGF-beta signaling and hepatic fibrosis. *Nat Med*. 2007; 13:1324–32. [PubMed: 17952090]
19. Satelli A, Li S. Vimentin in cancer and its potential as a molecular target for cancer therapy. *Cell Mol Life Sci*. 2011; 68:3033–46. [PubMed: 21637948]
20. de Leeuw AM, McCarthy SP, Geerts A, et al. Purified rat liver fat-storing cells in culture divide and contain collagen. *Hepatology*. 1984; 4:392–403. [PubMed: 6373550]
21. Van Rossen E, Vander Borgh S, van Grunsven LA, et al. Vinculin and cellular retinol-binding protein-1 are markers for quiescent and activated hepatic stellate cells in formalin-fixed paraffin embedded human liver. *Histochem Cell Biol*. 2009; 131:313–25. [PubMed: 19052772]
22. Muzumdar MD, Tasic B, Miyamichi K, et al. A global double-fluorescent Cre reporter mouse. *Genesis*. 2007; 45:593–605. [PubMed: 17868096]
23. Yang L, Jung Y, Omenetti A, et al. Fate-mapping evidence that hepatic stellate cells are epithelial progenitors in adult mouse livers. *Stem Cells*. 2008; 26:2104–13. [PubMed: 18511600]
24. Marra F. Chemokines in liver inflammation and fibrosis. *Front Biosci*. 2002; 7:d1899–914. [PubMed: 12161342]
25. Wasmuth HE, Tacke F, Trautwein C. Chemokines in liver inflammation and fibrosis. *Semin Liver Dis*. 2010; 30:215–25. [PubMed: 20665374]
26. Humphreys BD, Lin SL, Kobayashi A, et al. Fate tracing reveals the pericyte and not epithelial origin of myofibroblasts in kidney fibrosis. *Am J Pathol*. 2010; 176:85–97. [PubMed: 20008127]
27. Issa R, Zhou X, Constandinou CM, et al. Spontaneous recovery from micronodular cirrhosis: evidence for incomplete resolution associated with matrix cross-linking. *Gastroenterology*. 2004; 126:1795–808. [PubMed: 15188175]
28. Popov Y, Sverdlov DY, Sharma AK, et al. Tissue transglutaminase does not affect fibrotic matrix stability or regression of liver fibrosis in mice. *Gastroenterology*. 2011; 140:1642–52. [PubMed: 21277850]
29. Georges PC, Hui JJ, Gombos Z, et al. Increased stiffness of the rat liver precedes matrix deposition: implications for fibrosis. *Am J Physiol Gastrointest Liver Physiol*. 2007; 293:G1147–54. [PubMed: 17932231]
30. Olsen AL, Bloomer SA, Chan EP, et al. Hepatic stellate cells require a stiff environment for myofibroblastic differentiation. *Am J Physiol Gastrointest Liver Physiol*. 2011; 301:G110–8. [PubMed: 21527725]
31. Sancho-Bru P, Bataller R, Gasull X, et al. Genomic and functional characterization of stellate cells isolated from human cirrhotic livers. *J Hepatol*. 2005; 43:272–82. [PubMed: 15964095]
32. Kisseleva T, Cong M, Paik Y, et al. Myofibroblasts revert to an inactive phenotype during regression of liver fibrosis. *Proc Natl Acad Sci U S A*. 2012
33. Scholten D, Osterreicher CH, Scholten A, et al. Genetic labeling does not detect epithelial-to-mesenchymal transition of cholangiocytes in liver fibrosis in mice. *Gastroenterology*. 2010; 139:987–98. [PubMed: 20546735]

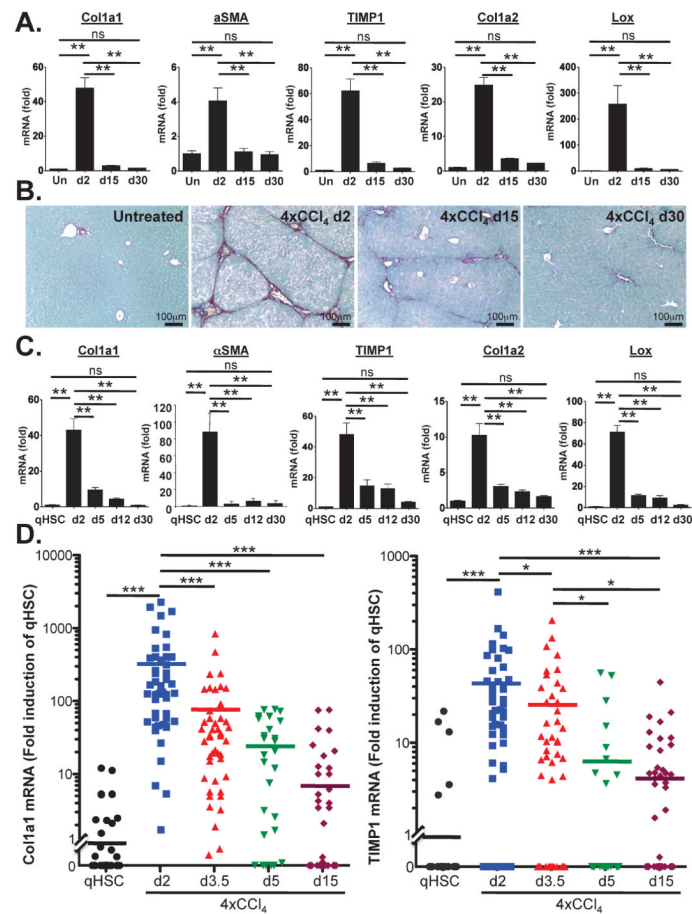


Figure 1. Analysis of CCl₄-induced HSC activation and deactivation by single cell qPCR
A–B. Fibrogenic gene expression (A.) and picosirius red staining (B.) was determined in livers of untreated Balb/c mice (n=4) or mice treated with 4 injections of CCl₄ (0.5 μl/g) and sacrificed 2 days (n=6), 15 days (n=5) or 30 days (n=8) after the last CCl₄ injection. Shown is a fold induction of mRNA levels compared to untreated controls (A) and representative pictures (B). **C.** Determination of fibrogenic gene expression in HSCs isolated from untreated Balb/c mice (n=4) or from Balb/c mice treated with 4 injections of CCl₄ (0.5 μl/g) and sacrificed either 2 days (n=3), 5 days (n=3), 12 days (n=3) or 30 days (n=5) after the last CCl₄ injection. **D.** Activation and deactivation was determined in single-cell FACS-sorted HSCs isolated from Balb/c untreated mice (n=58) or at various time points after 4 injections of CCl₄ (for d2 n=49, for d3.5 n=45, for d5 n=29, for d15 n=53). Shown is one of three representative HSC isolations for each time point. *p < 0.05, ** p<0.01, *** p<0.001

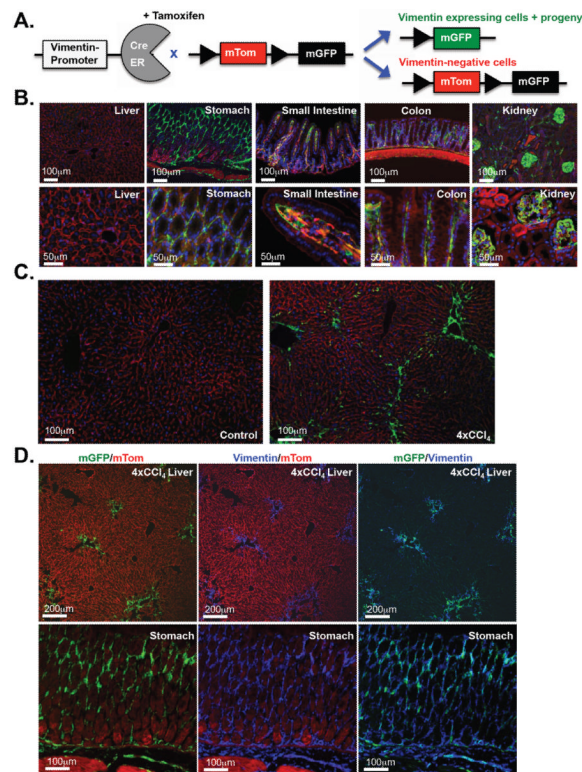


Figure 2. Vimentin-CreER marks vimentin-expressing cells in the intestinal tract and in the fibrotic liver

A. Schematic diagram showing mTom/mGFP reporter gene expression in the absence and presence of tamoxifen-inducible Cre-mediated recombination. **B.** Vim-CreER BAC-transgenic mice were crossed to mTom-mGFP Cre reporter mice and injected 6× with tamoxifen to visualize Cre-mediated recombination. Shown are representative sections of the liver, stomach, small intestine, colon and kidney with Cre-mediated recombination visible as green mGFP positive cells. **C.** Shown are representative sections of normal liver after 6 injections of tamoxifen and liver treated with 6 injections of tamoxifen and 4 injections of CCl₄. **D.** Livers from mice treated with 4 injections of CCl₄ or stomach from untreated mice were stained with anti-vimentin antibody and analyzed by confocal microscopy to demonstrate overlap between Vimentin-CreER induced mGFP expression (green) and endogenous vimentin expression (blue).

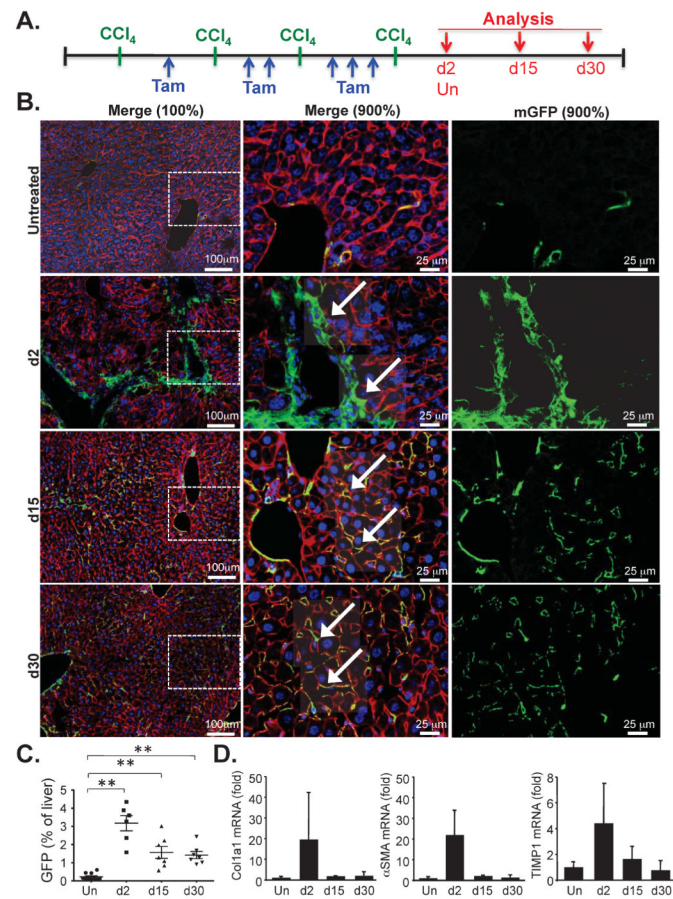


Figure 3. Hepatic myofibroblasts de-activate during regression of CCl₄-induced liver fibrosis
A. Schematic diagram showing the timing of tamoxifen and CCl₄ injections, and sacrifice of VimCreER mice. **B.** mGFP and mTom expression in livers of untreated or CCl₄-treated mice were visualized by confocal microscopy 2, 15 and 30 days after the last CCl₄ injection. The middle and right panel show higher magnification representing the area marked by dotted white lines in the left panel. **C.** mGFP expression was quantified and expressed as percentage of total area for mice receiving no CCl₄ (n=10), and CCl₄-treated mice at day 2 (n=6), day 15 (n=7) or day 30 (n=7) after the last CCl₄ injection. **D.** Fibrogenic gene expression in whole liver from Vim-CreER mice was performed by qPCR for mice receiving no CCl₄ (n=7), and CCl₄-treated mice at day 2 (n=4), day 15 (n=3) or day 30 (n=3) after the last CCl₄ injection. ** p<0.01

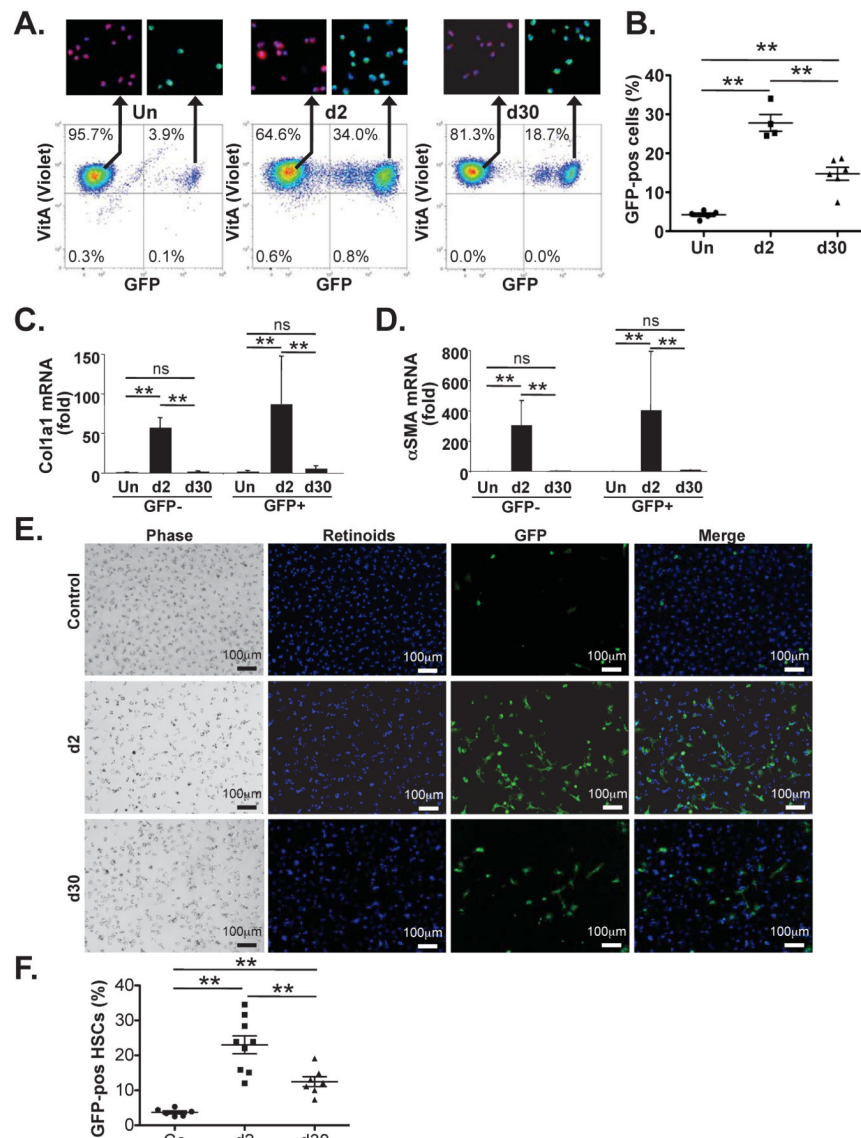


Figure 4. Hepatic stellate cells de-activate after cessation of liver injury

Vimentin-CreER mice were treated with 6 tamoxifen and 4 CCl₄ injections and HSCs were isolated 2 and 30 days after the last CCl₄ injection. HSCs from control mice receiving corn oil and tamoxifen were isolated at a time corresponding to 2 days after the last CCl₄ injection. **A–B.** mGFP expression was determined by flow-cytometric analysis of Vitamin A-autofluorescent HSCs. Shown are representative FACS images of each time point (A.) and quantification (B.) of HSCs from untreated mice (n=4), HSCs isolated 2 days (n=4) and 30 days (n=6) after the last CCl₄ injection. Inserts show HSCs from each sorted cell population confirming cells as vitamin A-positive HSCs expressing mTom but not mGFP, or mGFP but not mTom. **C–D.** qPCR for Col1a1 (C.) and αSMA (D.) was performed in mGFP-negative HSCs and mGFP-positive HSCs from untreated mice (n=5 each), mGFP-negative HSCs and mGFP-positive HSCs isolated from mice 2 days after 4×CCl₄ injection (n=4 each), and mGFP-negative HSCs and mGFP-positive HSCs isolated from mice 30 days after 4×CCl₄ injection (n=5 GFP-negative, n=4 GFP-positive). **E–F.** mGFP expression was determined by fluorescent microscopy of plated HSCs at various time points after CCl₄ and in control HSCs. Shown are representative pictures (E.) of vitamin A fluorescence, mGFP

expression and an overlay of both, and a quantification (F.) of GFP-positive/Vitamin A-positive HSCs isolated from untreated mice (n=6), HSCs isolated 2 days (n=9) and 30 days (n=7) after the last CCl₄ injection. ** p<0.01

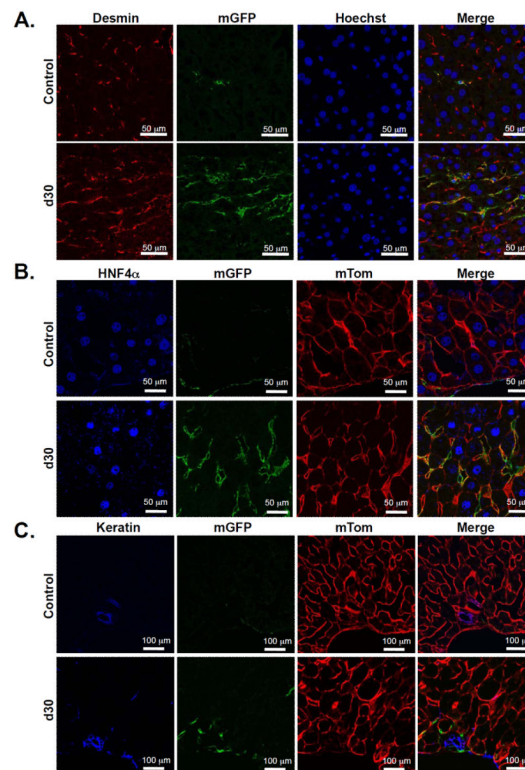


Figure 5. Hepatic myofibroblasts do not undergo mesenchymal-epithelial transition

A. To determine whether mGFP-labeled myofibroblast re-differentiate into HSCs, livers were stained for desmin and analyzed by confocal microscopy. Representative images show overlap between desmin (red) and mGFP in untreated mice and CCl₄-treated mice 31 days after the last tamoxifen injection. **B.** To determine whether mGFP-labeled myofibroblasts differentiate into hepatocytes, livers were stained with HNF4α. Confocal microscopy revealed no mGFP expressing cells with HNF4α-positive nuclei (blue). **C.** To determine whether mGFP-labeled myofibroblasts may differentiate into cholangiocytes, livers were stained with pankeratin antibody. Confocal microscopy revealed no overlap between pankeratin-positive bile ducts (blue) and mGFP (green).

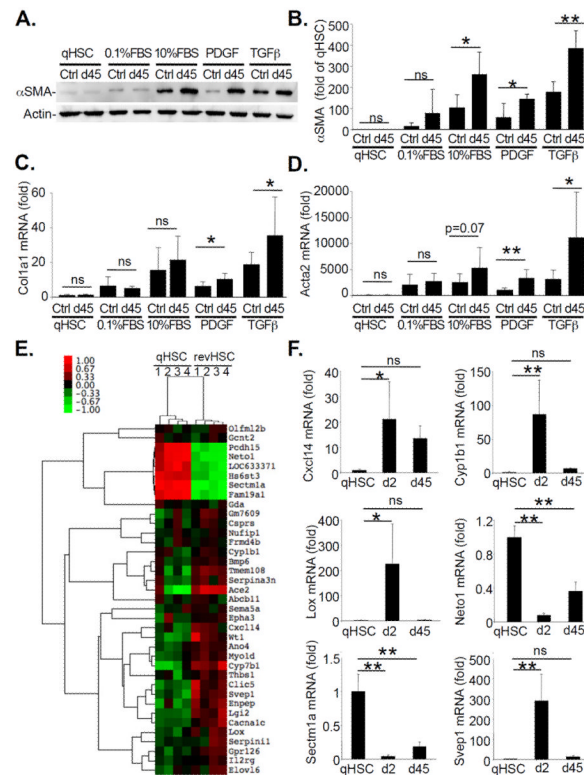


Figure 6. Reverted HSCs are more responsive to fibrogenic stimuli

HSCs were isolated from age-matched mice that were left untreated or mice that received 4 injections of CCl₄ (0.5 μl/g i.p.), followed by 45 days without treatment. **A–B.** Shown is a representative αSMA immunoblot of untreated HSCs (Ctrl) and d45 reverted HSCs (d45) using unplate freshly isolated quiescent HSCs (qHSC), HSCs cultured for 48h in 0.1% FBS-containing media, HSCs cultured for 48h in 10% FBS-containing media, or HSCs cultured treated with PDGF (20 ng/ml) or TGFβ (2 ng/ml) in 0.1% FBS-containing media, and a densitometric analysis (B) of αSMA immunoblots from 5 independent HSC isolations per group, normalized to actin levels. **C–D.** Shown are qPCR results for fibrogenic markers Col1a1 (C) and Acta2 (D) using the above-described samples of control and d45 reverted HSCs. **E.** Microarray analysis comparison of qHSCs and reverted HSCs, isolated from mice that received 4 injections of CCl₄ (0.5 μl/g i.p.), followed by 45 days without treatment. Shown are all genes with a corrected p-value of <0.05 and a log fold-change of at least 0.67. **F.** qPCR of genes selected from the above microarray comparing expression levels of HSCs isolated from untreated mice (n=4), d2 after 4×CCl₄ treatment (n=3) and d45 after 4×CCl₄ treatment (n=4). Shown is a fold in comparison to qHSCs isolated from untreated mice. * p<0.05. ** p<0.01